Desalination and Water Treatment
www.deswater.com

doi: 10.5004/dwt.2017.20891

80 (2017) 247–254
June

Thermodynamic, kinetic and isotherm studies of sulfate removal from aqueous solutions by graphene and graphite nanoparticles

Ali Naghizadeh[a,b,c,*], Fatemeh Ghasemi[a], Elham Derakhshani[a], Habibeh Shahabi[a]

[a]*Medical Toxicology and Drug Abuse Research Center (MTDRC), Birjand University of Medical Sciences (BUMS), Birjand, Iran, Tel. +9856132381665; Fax: +9856132381132; emails: aliinaghizadeh@gmail.com (A. Naghizadeh), fatemehghasemi69@yahoo.com (F. Ghasemi), el.derakhshani@yahoo.com (E. Derakhshani), habibeh.shahabi@yahoo.com (H. Shahabi)*
[b]*Department of Environmental Health Engineering, Faculty of Health, Birjand University of Medical Sciences (BUMS), Birjand, Iran*
[c]*Social Determinants of Health Research Center, Birjand University of Medical Sciences (BUMS), Birjand, Iran*

Received 15 August 2016; Accepted 2 May 2017

ABSTRACT

Sulfur compounds exist in the wastewater of industries like paper-making, food processing, photography, etc. Higher levels of sulfate in drinking water lead to its bitter taste and digestive problems as well as corrosion of sewer pipes in addition to causing problems in the anaerobic wastewater treatment processes. Based on this, the present study investigates the equilibrium, kinetics, thermodynamics and isotherms of sulfate removal process by graphene and graphite nanoparticles. This study explored the effects of the parameters including pH, adsorbent dosage, and initial concentration of sulfate, as well as the impacts of contact time and temperature on sulfate removal process in a batch system. The isotherms, thermodynamics and kinetics of the process were also studied. In this study, UV/VIS Spectrometer T80 was used to measure the sulfate concentration. The results obtained from the investigation of the efficiency of graphite and graphene nanoparticles demonstrated that these nanoparticles had the highest adsorption capacity at the acidic pH = 3, adsorbent dose of 0.2 g L^{-1} and sulfate concentration of 75 mg L^{-1}. The process of adsorption in graphene and graphite nanoparticles was found to follow the Freundlich isotherm model and pseudo-second-order kinetic model. The results also revealed that sulfate adsorption process with the studied nanoparticles was endothermic. Compared with graphene nanoparticles, the results indicate that graphite nanoparticles have more efficiency in removal of sulfate from aqueous solution. Moreover, the highest removal efficiency by graphene and graphite nanoparticles occurs in higher concentrations of sulfate. Therefore, the two nanoadsorbents can be used in adsorbing sulfate from the aqueous solutions.

Keywords: Sulfate; Graphene nanoparticles; Graphite nanoparticles; Thermodynamic; Isotherm

1. Introduction

Sulfate is one of the common pollutants which can be found both in natural water and wastewater [1–3]. Besides being available as insoluble salts, it also exists in the form of soluble compounds in the seas and oceans. Industrial wastewater is responsible for much of the sulfate emissions to the environment [2]. Decomposition of sulfate minerals and of plant and animal remains is the most important natural sources of sulfate emissions [4–6]. Household wastewaters usually have a sulfate concentration ranging from 20 to 500 mg L^{-1} [7], while industrial wastewaters may contain several thousand milligrams per liter of this pollutant [1,5,8,9]. Sulfur compounds also exist in the wastewater of other industries such as paper making industry, food processing, photography, etc. The damage caused by the release of sulfate is not direct because it is a neutral, non-volatile and non-toxic compound [2]. However, high concentrations of sulfate can cause imbalance in the natural cycle of sulfur [1,7]. Accumulation of sulfate-rich sediments in lakes, seas

* Corresponding author.

and rivers can result in toxic sulfide emissions in the environment [10]. High levels of sulfate in drinking water can make the taste of water bitter and cause gastrointestinal problems [5]. It can also lead to corrosion in sewer pipes and cause problems in anaerobic wastewater treatment processes [9,11]. According to the WHO, the normal level of sulfate in drinking water is 250 mg L^{-1} [12]. Although the health effects of sulfate last for a relatively short time, these effects are acute and sulfate concentrations should be reduced to the recommended dose [13]. Several methods have been suggested to remove sulfate from the aqueous solutions including reverse osmosis, electrodialysis or nanofiltration most of which are highly expensive and associated with high operating costs, increased sodium salts, the need for final treatment and disposal of wastewater sludge, etc. [9,11,14,15]. Ion exchange, biological purification, adsorption and chemical precipitation processes are also among the processes used for the treatment of sulfate-rich wastewater [2]. Adsorption by nanomaterials was the method employed in this study.

Adsorbents are widely used in water treatment and removal of inorganic and organic pollutants from contaminated water and this is more effective in removing contaminants from water than the other methods. Also, adsorption is considered a fast and inexpensive purification method [15–20]. Among adsorbents, carbon is convenient and varied element that in different patterns on the nanoscale can be used to remove contaminants.

Nanoparticles have two important features that make them suitable as adsorbents. First, they have significantly wider surface areas than other particles. Furthermore, they can be combined with different chemical groups to increase their tendency to remove the target compounds [21,22].

Adsorbents that are used in this study are graphene and graphite nanoparticles. Graphene due to extraordinary properties of electrical conductivity and thermal conductivity, high density, mobility of charge carriers, optical conductivity and mechanical properties of the material become more suitable for environmental uses. The length of carbon–carbon bonds in graphene particles was about 0.142 nm. The underlying structure for the production of carbon nanostructures, single-layer graphene is that if place on each other make up pile three-dimensional graphite [23–25]. Graphite nanoparticles belong to the large family of promising nanoscale carbon materials with carbon honeycomb net. Graphite material with high conductivity, good chemical resistance in ambient temperature provides good resistance to acid and alkali solution. Graphite nanoparticles, due to the nanostructure, have the character of good electrical properties, enough specific surface, large surface energy, apart from the general character of the graphite. Graphite nanoparticles is cheaper and easier to produce and can be easily constructed with large quantities than single-walled carbon nanotubes and graphene oxide [26].

Moreover, as one of the major problems of the water in southern Khorasan Province of Iran is the high level of sulfate that runs the risk of gastrointestinal disorders and since sulfate transferred to wastewater causes an offensive odor in Birjand municipal wastewater treatment plant, the present study tried to investigate sulfate removal at a pilot scale in the batch system using the given nanomaterials. Although many studies have been performed on the removal of sulfate, no published study has yet explored the application of graphene and graphite nanoparticles for removing sulfate.

2. Materials and methods

This experimental research was an applied investigation which was conducted on a batch scale. Adsorbents used in this study included graphene and graphite nanoparticles which were purchased from the Iranian Research Institute of Petroleum Industry (Iran) which produced by chemical vapor deposition (CVD) technique. Other chemical compounds used were purchased from Merck company (USA) with laboratory grade. To make stock solution, sodium sulfate was used. Additionally, sodium hydroxide and hydrochloride acid were utilized to adjust pH. Sulfate stock solution with 500 mg L^{-1} of concentration was made by solving a certain amount of sodium sulfate (as per its molecular weight and purity percentage) in double-distilled water. In this study, various parameters such as initial concentration of sulfate, adsorbent dose, contact time and pH were investigated. The Erlenmeyer flasks as reactor which contained different doses of graphene and graphite nanoparticles (0.2, 0.4, 0.6, 0.8 and 1 g L^{-1}) and 50 mL sulfate solution with different concentrations (25, 35, 50, 75 and 100 mg L^{-1}) were placed on the shaker at each stages. The pH ranged from 3, 5, 7, 9 to 11 and the mixture speed, with a time scale varying from 5, 10, 20, 30 to 40 min, was 250 rpm. Following this stage, the samples were filtered and the sulfate concentration was measured using the spectrophotometer (T80 UV–VIS Spectrometer) at a wavelength of 420 nm based on the procedure set out in the book of standard method. The experiments were repeated twice and the results offered demonstrated the mean for the obtained data. The sulfate adsorption capacity by graphite and graphene nanoparticles were calculated by the following formula:

$$q_e = \frac{(C_0 - C_e)}{M} \times V \quad (1)$$

where C_0 and C_e are the initial and final concentration of sulfate (mg L^{-1}), respectively, M is the weight of adsorbent (g) and V is the volume of solution (L).

3. Results and discussion

3.1. Characteristics of the adsorbents

Scanning electron microscopy (SEM) has been performed to investigate the morphologies of graphite and graphene nanosheets. SEM analysis of Fig. 1(a) revealed that the graphene nanosheets are stacks of multi-layered graphene sheets having a platelet morphology which have large, transparent graphene sheets with few layers [27]. Fig. 1(b) shows the SEM image for graphite nanosheets. According to this figure, these nanoparticles consist of irregular morphology with the size of a few micrometers [28,29].

According to information of nanoparticles producer company, nanographene has less than 32 layers for which the thicknesses of the layers are in the ranges of 2–18 nm. Also the nanographite particles are very intact with the matrix material for which the thickness of the layers is about 5–20 nm.

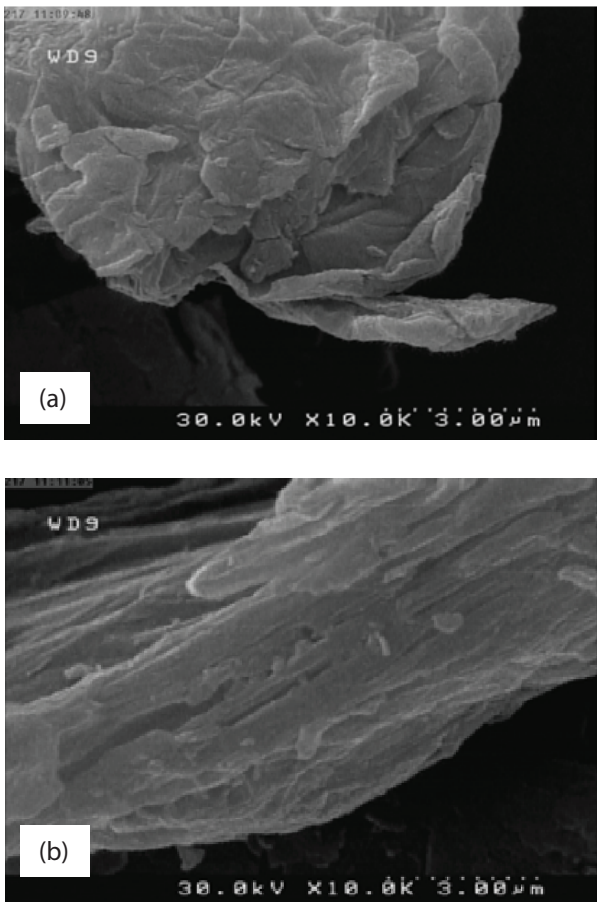

Fig. 1. SEM images of (a) graphene and (b) graphite nanoparticles.

The XRD patterns of graphite and nanographene are shown in Fig. 2. As can it be seen, the XRD pattern of the graphite (Fig. 2(a)) sample clearly displays a high degree of crystallinity, with a strong and sharp diffraction peak at around 26° which can be indexed to the reflection (002) of the graphite. In addition, a slight diffraction peak appears at 54° corresponding to the (004) plane of the graphite [28].

The XRD patterns of nanographite in Fig. 2(b) shows that the distinguishable (002) peak of graphite at 26.56° has an interlayer distance of 0.334 nm (002). This implies that nanographite is a highly oriented carbon material [30].

3.2. Determining the effects of pH on sulfate adsorption by graphite and graphene nanoparticles

The results obtained from the investigation of the impact of pH on graphite and graphene nanoparticles are shown in Fig. 3.

The pH factors play an important role in the adsorption process through their influence on adsorption load, ionization of solution components and separation of functional groups of the material on the surface of active zones of the adsorbent [31]. As is evident in Fig. 3, the highest adsorption capacity for graphite and graphene nanoparticles occurred at pH = 3 which are 4.53 and 3.67 mg g^{-1}, respectively. Namely, with an increase in pH, sulfate adsorption decreased in both nanoparticles. This was due to the adsorbents surface charge

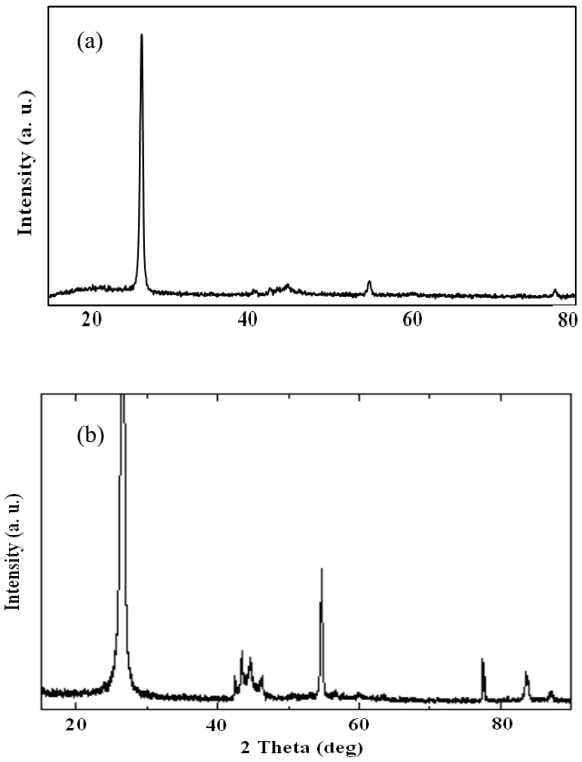

Fig. 2. XRD pattern of (a) nanographene and (b) nanographite.

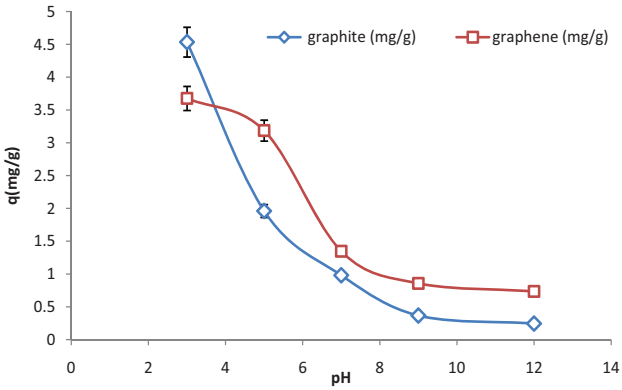

Fig. 3. Effect of pH on the adsorption of sulfate by graphite and graphene nanoparticles.

and sulfate anion loading. By reducing pH, the positive charges around the adsorbents are increased which leads to increased adsorption of sulfate on the surface of adsorbents [32].The results of this study correspond with the results of a study by Boukhalfa et al. [3]. The findings of another study performed by Shams et al. [33] showed a better performance of acidic pH in sulfate removal. Lyang et al. [34] showed that the optimized pH for sulfate removal was 4.5.

3.3. The effect of the initial concentration of sulfate on its adsorption by graphene and graphite nanoparticles at different times

The results of the investigation related to the initial concentration of sulfate adsorption by graphene and graphite nanoparticles at various time scales are given in Figs. 4 and 5.

Figs. 4 and 5 show the adsorption capacity of different concentrations of sulfate at different times by graphene and graphite nanoparticles. Based on Fig. 5, the highest sulfate adsorption capacity occurred at 75 mg L^{-1} of concentration within 20 min which amounted to 20.83 mg g^{-1} and following which the adsorption level reached a partial equilibrium. In this figure, the sulfate adsorption capacities at concentrations of 25, 35, 50 and 75 mg L^{-1} after 20 min were 8.57, 9.92, 10.48 and 20.83 mg g^{-1}, respectively. As it can be seen, the adsorption capacity in this figure has increased up to 20 min in all the concentrations.

In Fig. 5, the highest adsorption rate was seen at a concentration of 75 mg L^{-1} (i.e., 4.41 mg g^{-1}) at 30 min of time following which adsorption reached equilibrium. The sulfate adsorption capacities in Fig. 5 at concentrations of 25, 35, 50 and 75 mg L^{-1} after 30 min were 2.29, 2.68, 3.89 and 4.41 mg g^{-1}, respectively. In this figure, the sulfate adsorption capacity has had an increasing trend for 30 min at all concentrations and then it achieved equilibrium.

As can be seen, increasing concentrations of sulfate leads to its enhanced adsorption by graphene and graphite nanoparticles. This might be because of the existence of free adsorbent bands and ion exchange bands at low concentrations of sulfate [35]. As it is evident, enhanced contact time increases the adsorption rate which can be due to frequent contact between the adsorbent and pollutants [36–38]. The equilibrium in adsorption capacity may also be due to the occupation of the adsorption free surface. The result drawn from the two figures is that the graphite nanoparticles have a higher ability in sulfate adsorption compared with graphene nanoparticles. The results of a study performed by Wang et al. [39] showed that the removal of folic acid by modified zeolite was increased with enhanced concentration until it reached equilibrium within 120 min. In an investigation conducted by Khalatbari and Bazgir [40], sulfate adsorption reached equilibrium in 90 min and adsorption level was shown to increase with enhanced sulfate. The results of the study conducted by Shams et al. [33] showed that increasing contact time increases sulfate removal and that maximum removal occurs during the initial primary stages of the experiment.

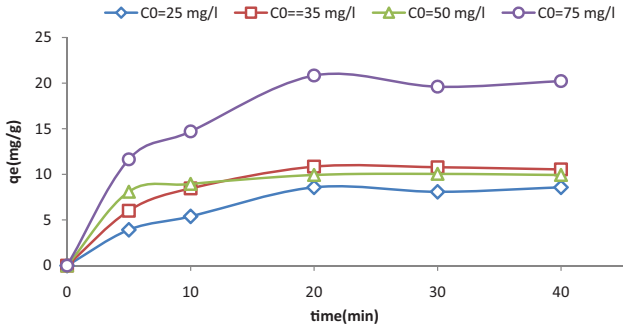

Fig. 4. Effect of initial sulfate concentration on the adsorption capacity of graphite nanoparticles at different contact times.

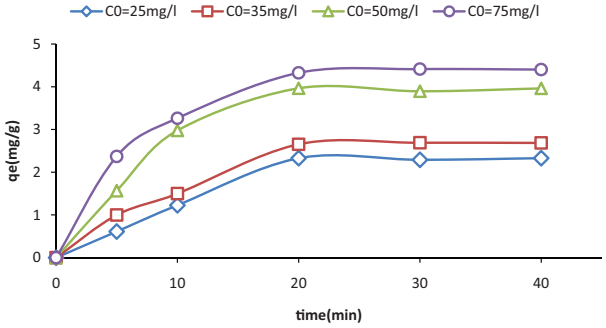

Fig. 5. Effect of initial sulfate concentration on the adsorption capacity of graphene nanoparticles at different contact times.

3.4. The effect of graphene and graphite nanoparticles dosage on sulfate adsorption

Fig. 6 shows the amounts of sulfate adsorption in graphene and graphite nanoparticles adsorbents with dosages of 0.2, 0.4, 0.6, 0.8 and 1 g L^{-1}. According to this figure, the adsorption capacities of graphene and graphite nanoparticles at dosage of 0.2 g L^{-1} and retention time of 30 min and sulfate concentration of 75 mg L^{-1} were 16.54 and 18.38 mg g^{-1}, respectively. As a result, in the given adsorbents, the adsorption capacities reduced as adsorbent dosage increased but sulfate removal efficiencies increased with increasing adsorbent masses. Increased sulfate adsorption due to the increase in the mass of adsorbent results from the increase in the effective and active surface for adsorption. Although increase in adsorbent dosage leads to higher removal of sulfate, due to incomplete saturation of adsorbent surface and lack of its use, the adsorption capacity decreases per mass unit [41,42]. Such a finding has also been confirmed in studies performed by Dehghani et al. [43] concerning the removal of RB29 using carbon nanotubes.

3.5. Investigating isotherm models of adsorption

In this section, the results of two most widely used isotherm models, that is, Freundlich and Langmuir are given in Figs. 7 and 8 and a summary of the results are presented in Table 1.

Adsorption isotherms are used to define the behavior of the adsorbate concentration on the adsorbent. Isotherm indicates how pollutants react with the adsorbent. The type of isotherm can provide information such as the nature of adsorbate and adsorbent surface. Furthermore, it is useful in describing the adsorption capacity and analyzing and designing the adsorption systems [44]. Langmuir and Freundlich are among the most commonly used models of isotherm

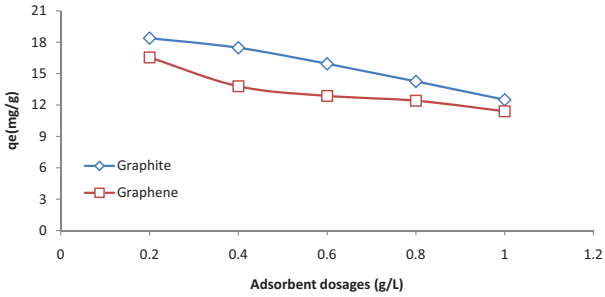

Fig. 6. Effect of graphite and graphene nanoparticles dosage on sulfate adsorption.

[45,46]. In this study, the two given isotherms were used to analyze adsorption data. An investigation of Langmuir and Freundlich isotherms indicated that both follow Freundlich isotherm model as regards the highest coefficient correlation of these two adsorbents. Freundlich equation is expressed in terms of physical adsorption between pollutants and adsorbents, and assumes that adsorption taking place is multi-layered. It cannot predict the maximum adsorption of pollutants on the sorbent surface [47,48]. A study by Cao et al. [49] showed that sulfate removal by rice straws follows the Langmuir isotherm model.

3.6. Effect of temperature on adsorption process and determination of thermodynamic parameters

The thermodynamic parameters include enthalpy changes ($\Delta H°$), entropy changes ($\Delta S°$) and Gibbs free energy changes ($\Delta G°$). These parameters needed to be determined to show the spontaneous nature of the adsorption process.

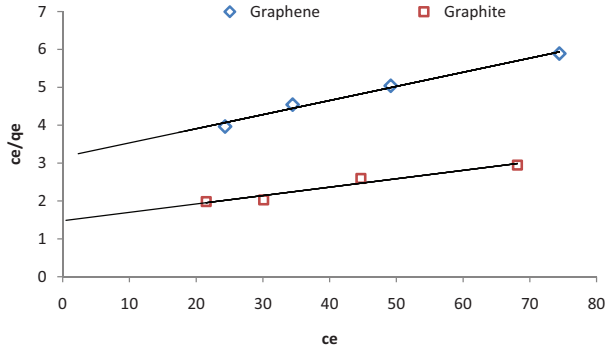

Fig. 7. Langmuir isotherm for the graphene and graphite nanoparticles.

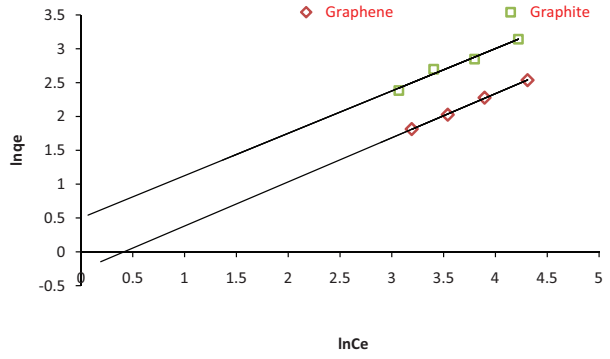

Fig. 8. Freundlich isotherm for the graphene and graphite nanoparticles.

The spontaneous process occurs when $\Delta G°$ is negative [20,50]. In this study, the thermodynamic parameters were considered at different temperatures (293, 303 and 313 K) and all the thermodynamic parameters were calculated using the following formula [20]:

$$K_c = \frac{C_{Ad}}{C_e} \tag{2}$$

$$\Delta G° = -RT \ln K_c \tag{3}$$

$$\ln K_c = \frac{\Delta S°}{R} - \frac{\Delta H°}{RT} \tag{4}$$

Fig. 9 and Table 2 show the results of the effects of temperature on sulfate adsorption process by graphite and graphene nanoparticles.

According to Table 2 which shows positive $\Delta H°$ values for graphene and graphite nanoparticles (18.55 and 21.10 kJ mol^{-1}, respectively), the process of sulfate adsorption by graphite and graphene nanoparticles was endothermic. A study by Runtti et al. [51] on sulphate removal also revealed the endothermic process of removal. In another study conducted by Ganesan et al. [18] on the adsorption of nitrate ions on graphene represents the adsorption process was endothermic. Also, the $\Delta G°$ parameter is positive and decreases along with increasing temperature. Therefore, this adsorption process is not spontaneous, and external energy would be required to promote the adsorption process.

In the present study, the entropy ($\Delta S°$) values were positive for graphene and graphite nanoparticles (57.60 and 69.59 J mol^{-1} K^{-1}, respectively) as well. In other words, the positive entropy represents an increase in the removal efficiency with increase in temperature [51].

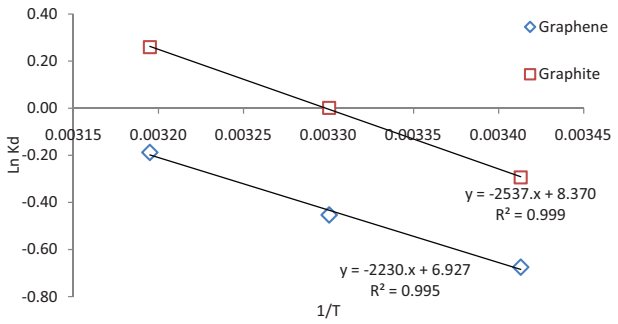

Fig. 9. Effect of temperature on adsorption of sulfate by graphite and graphene nanoparticles.

Table 1
Results of isotherms (Langmuir and Freundlich)

Nanoparticles	Langmuir			Freundlich		
	K_L (L mg^{-1})	q_m (mg g^{-1})	R^2	k_f	n	R^2
Graphite	30.51	45.06	0.95	1.64	1.59	0.97
Graphene	8.48	26.83	0.98	0.76	1.53	0.99

3.7. Kinetic study of adsorption

The results of the kinetic study of sulfate adsorption by graphite and graphene nanoparticles are shown in Figs. 10–13 and Table 3.

Kinetic studies are among important investigations on adsorption in which the effect of contact time on the adsorption capacity is considered [52,53]. Furthermore, the kinetic studies of adsorption are useful for the prediction of adsorption rate which provides useful information for modeling and designing the process. As regards, the results of kinetic investigations of sulfate adsorption by graphene and graphite nanoparticles that are shown in Table 3 for sulfate concentrations of 25, 35, 50 and 75 mg L^{-1}, the pseudo-second-order kinetic model is selected for both graphene and graphite nanoparticles in all concentrations. According to these results, the equilibrium capacity of adsorption increases as the concentration of the pollutant increases, and adsorption has a higher efficiency at higher concentrations. The result of this study confirms the findings of a study conducted by Runtti et al. [54] concerning the utilization of barium-modified analcime in sulphate removal. Results of another study conducted by Ganesan et al. [19] corresponded to with the results of our study.

4. Conclusion

In this study, removal of sulfate ions from aqueous solutions by graphene and graphite nanoparticles was studied. The results demonstrated that these nanoparticles had the highest adsorption capacity at the acidic pH, adsorbent dose of 0.2 g L^{-1} and sulfate concentration of 75 mg L^{-1}. The process of adsorption in both nanoparticles was found to follow the both Freundlich and Langmuir isotherms and pseudo-second-order kinetic model. The findings also

Table 2
Effect of temperature on adsorption process and thermodynamic parameters

Nanoparticles	T (K)	q_e (mg g^{-1})	Thermodynamics parameters		
			ΔG (kJ mol^{-1})	ΔH (kJ mol^{-1})	ΔS (J mol^{-1} K^{-1})
Graphene	293	37.9	1.64	18.54	57.60
	303	46.25	1.14		
	313	58.3	0.49		
Graphite	293	53.19	0.72	21.10	69.59
	303	68.4	0.00		
	313	84.4	–0.67		

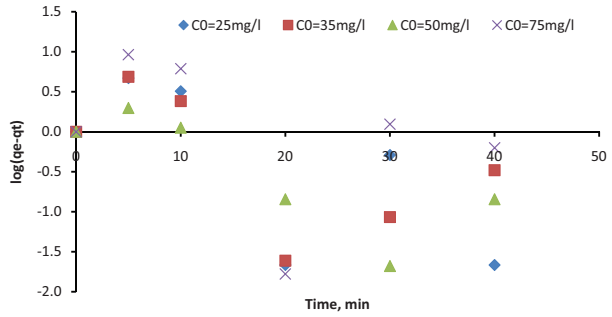

Fig. 10. Pseudo-first-order kinetic plot for sulfate adsorption by graphite nanoparticles.

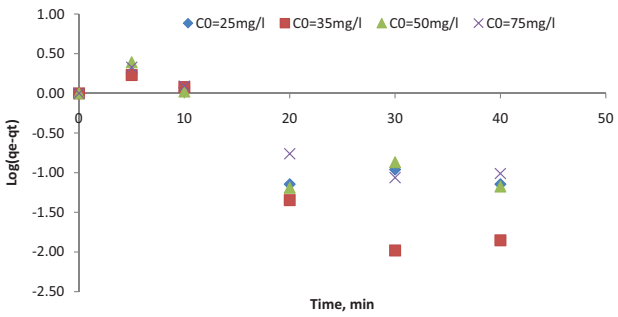

Fig. 11. Pseudo-first-order kinetic plot for sulfate adsorption by graphene nanoparticles.

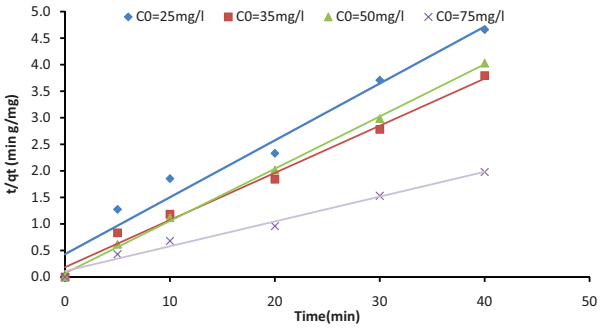

Fig. 12. Pseudo-second-order kinetic plot for sulfate adsorption by graphite nanoparticles.

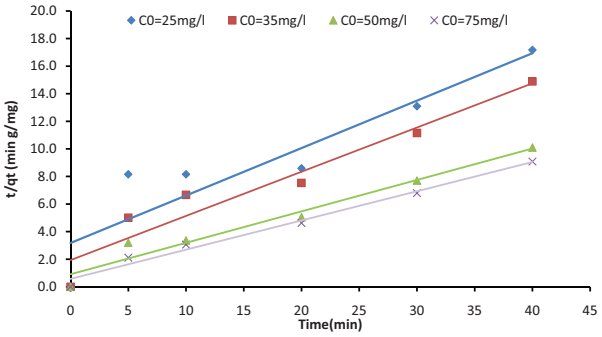

Fig. 13. Pseudo-second-order kinetic plot for sulfate adsorption by graphene nanoparticles.

Table 3
Pseudo-first-order and pseudo-second-order equations for sulfate adsorption by nanographene and nanographite

Nanoparticles	C_0 (mg L^{-1})	Pseudo-first-order			Pseudo-second-order			$q_{e,}$ exp (mg g^{-1})
		K_1 (min^{-1})	$q_{e,}$ cal (mg g^{-1})	R^2	K_2 (g mg min^{-1})	$q_{e,}$ cal (mg g^{-1})	R^2	
Graphite	25	0.11	2.75	0.52	0.03	9.33	0.96	8.60
	35	0.08	1.72	0.34	0.04	11.26	0.99	10.87
	50	0.09	1.50	0.63	0.14	10.16	0.99	10.07
	75	0.05	2.28	0.12	0.02	21.37	0.98	20.85
Graphene	25	0.09	1.46	0.75	0.04	2.91	0.85	2.40
	35	0.14	1.86	0.86	0.05	3.12	0.93	2.70
	50	0.09	1.58	0.73	0.06	4.38	0.91	4.03
	75	0.08	1.69	0.82	0.08	4.72	0.99	4.50

revealed that sulfate adsorption process was endothermic. The results indicated that graphite nanoparticles have more efficiency in removing sulfate than graphene nanoparticles.

Acknowledgments

This article is the project approved in Deputy of Research of Birjand University of Medical Sciences, Therefore, the author is grateful to the Deputy of Research of Birjand University of Medical Sciences for the financial support as well as all the laboratory staffs of Department of Environmental Health Engineering.

References

[1] A.J. Silva, M.B. Varesche, E. Foresti, M. Zaiat, Sulphate removal from industrial wastewater using a packed-bed anaerobic reactor, Process Biochem., 37 (2002) 927–935.
[2] C.T. Benatti, C.l.R.G. Tavares, E. Lenzi, Sulfate removal from waste chemicals by precipitation, Environ. Manage., 90 (2009) 504–511.
[3] C. Boukhalfa, A. Mennour, L. Reinert, H. Fuzellier, Sulfate removal from aqueous solutions by hydrous iron oxide macroscopic, thermal and spectroscopic analyses, Desalination, 214 (2007) 38–48.
[4] A. Wiessner, U. Kappelmeyer, P. Kuschk, M. Kästner, Sulphate reduction and the removal of carbon and ammonia in a laboratory-scale constructed wetland, Water Res., 39 (2005) 4643–4650.
[5] C. Namasivayam, D. Sangeetha, Application of coconut coir pith for the removal of sulfate and other anions from water, Desalination, 219 (2008) 1–13.
[6] D.R. Mulinari, M.L.C.C.P. da Silva, Adsorption of sulphate ions by modification of sugarcane bagasse cellulose, Carbohydr. Polym., 74 (2008) 617–620.
[7] P.N.L. Lens, A. Visser, A.J.H. Janssen, L.W.H. Pol, G. Lettinga, Biotechnological treatment of sulfate-rich wastewaters, Crit. Rev. Environ. Sci. Technol., 28 (1998) 41–88.
[8] M.V. Galiana-Aleixandre, A. Iborra-Clar, B. Bes-PiÃ¡, J.A. Mendoza-Roca, B. Cuartas-Uribe, M.I. Iborra-Clar, Nanofiltration for sulfate removal and water reuse of the pickling and tanning processes in a tannery, Desalination, 179 (2005) 307–313.
[9] S. Tait, W.P. Clarke, J. Keller, D.J. Batstone, Removal of sulfate from high-strength wastewater by crystallisation, Water Res., 43 (2009) 762–772.
[10] R. Ghigliazza, A. Lodi, M. Rovatti, Kinetic and process considerations on biological reduction of soluble and scarcely soluble sulfates, Resour. Conserv. Recycl., 29 (2000) 181–194.
[11] E. Sahinkaya, Microbial sulfate reduction at low (8 °C) temperature using waste sludge as a carbon and seed source, Int. Biodeterior. Biodegrad., 63 (2009) 245–251.
[12] E.W. Rice, L. Bridgewater, American Public Health Association, Standard Methods for the Examination of Water and Wastewater, APHA, Washington, D.C., 2014.
[13] K. Košutić, I. Novak, L. Sipos, B. Kunst, Removal of sulfates and other inorganics from potable water by nanofiltration membranes of characterized porosity, Sep. Purif. Technol., 37 (2004) 177–185.
[14] A. Wang, N. Ren, X. Wang, D. Lee, Enhanced sulfate reduction with acidogenic sulfate-reducing bacteria, J. Hazard. Mater., 154 (2008) 1060–1065.
[15] R. Kamaraj, S. Vasudevan, Decontamination of selenate from aqueous solution by oxidized multi-walled carbon nanotubes, Powder Technol., 274 (2015) 268–275.
[16] M.R. Gandhi, S. Vasudevan, A. Shibayama, M. Yamada, Graphene and graphene-based composites: a rising star in water purification - a comprehensive overview, ChemistrySelect, 1 (2016) 4358–4385.
[17] R. Kamaraj, P. Ganesan, S. Vasudevan, Use of hydrous titanium dioxide as potential sorbent for the removal of manganese from water, J. Electrochem. Sci. Eng., 4 (2014) 187–201.
[18] P. Ganesan, R. Kamaraj, S. Vasudevan, Application of isotherm, kinetic and thermodynamic models for the adsorption of nitrate ions on graphene from aqueous solution, J. Taiwan Inst. Chem. Eng., 44 (2013) 808–814.
[19] P. Ganesan, R. Kamaraj, G. Sozhan, S. Vasudevan, Oxidized multiwalled carbon nanotubes as adsorbent for the removal of manganese from aqueous solution, Environ. Sci. Pollut. Res., 20 (2013) 987–996.
[20] J. Lakshmi, S. Vasudevan, Graphene – a promising material for removal of perchlorate (ClO_4–) from water, Environ. Sci. Pollut. Res., 20 (2013) 5114–5124.
[21] N. Savage, M.S. Diallo, Nanomaterials and water purification: opportunities and challenges, J. Nanopart. Res., 7 (2005) 331–342.
[22] A. Naghizadeh, Comparison between activated carbon and multiwall carbon nanotubes in the removal of cadmium(II) and chromium(VI) from water solutions, J. Water Supply Res. Technol. AQUA, 64 (2015) 64–73.
[23] R.R. Nair, P. Blake, A.N. Grigorenko, K.S. Novoselov, T.J. Booth, T. Stauber, N.M.R. Peres, A.K. Geim, Fine structure constant defines visual transparency of graphene, Science, 320 (2008) 1308–1308.
[24] K.S.A. Novoselov, A.K. Geim, S. Morozov, D. Jiang, M. Katsnelson, I. Grigorieva, S. Dubonos, A. Firsov, Two-dimensional gas of massless Dirac fermions in graphene, Nature, 438 (2005) 197–200.
[25] K.S. Novoselov, D. Jiang, F. Schedin, T.J. Booth, V.V. Khotkevich, S.V. Morozov, A.K. Geim, Two-dimensional atomic crystals, Proc. Natl. Acad. Sci. USA, 102 (2005) 10451–10453.
[26] X. Guo, D. Li, J. Wan, X. Yu, Preparation and electrochemical property of TiO_2/nano-graphite composite anode for electro-catalytic degradation of ceftriaxone sodium, Electrochim. Acta, 180 (2015) 957–964.
[27] K. Kakaei, One-pot electrochemical synthesis of graphene by the exfoliation of graphite powder in sodium dodecyl sulfate and its decoration with platinum nanoparticles for methanol oxidation, Carbon, 51 (2013) 195–201.

[28] K. Kakaei, K. Hasanpour, Synthesis of graphene oxide nanosheets by electrochemical exfoliation of graphite in cetyltrimethylammonium bromide and its application for oxygen reduction, J. Mater. Chem. A, 2 (2014) 15428–15436.
[29] K. Kakaei, M. Dorraji, One-pot synthesis of Palladium Silver nanoparticles decorated reduced graphene oxide and their application for ethanol oxidation in alkaline media, Electrochim. Acta, 143 (2014) 207–215.
[30] I. Karteri, S. karataş, A. Al-Ghamdic, F. Yakuphanoğlu, The electrical characteristics of thin film transistors with graphene oxide and organic insulators, Synth. Met., 199 (2015) 241–245.
[31] S. Chowdhury, R. Mishra, P. Saha, P. Kushwaha, Adsorption thermodynamics, kinetics and isosteric heat of adsorption of malachite green onto chemically modified rice husk, Desalination, 265 (2011) 159–168.
[32] H. Runtti, S. Tuomikoski, T. Kangas, T. Kuokkanen, J. Rama, U. Lassi. Sulphate removal from water by carbon residue from biomass gasification: effect of chemical modification methods on sulphate removal efficiency, BioResources, 11 (2016) 3136–3152.
[33] M. Shams, M. Qasemi, M. Afsharnia, A. Hossein Mahvi, Sulphate removal from aqueous solutions by granular ferric hydroxide, Desal. Wat. Treat., 57 (2016) 23800–23807.
[34] F. Liang, Y. Xiao, F. Zhao, Effect of pH on sulfate removal from wastewater using a bioelectrochemical system, Chem. Eng. J., 218 (2013) 147–153.
[35] C.-H. Wu, Adsorption of reactive dye onto carbon nanotubes: equilibrium, kinetics and thermodynamics, J. Hazard. Mater., 144 (2007) 93–100.
[36] E.S. El-Ashtoukhy, N.K. Amin, O. Abdelwahab, Removal of lead (II) and copper (II) from aqueous solution using pomegranate peel as a new adsorbent, Desalination, 223 (2008) 162–173.
[37] E. Derakhshani, A. Naghizadeh, Ultrasound regeneration of multiwall carbon nanotubes saturated by humic acid, Desal. Water Treat., 52 (2014) 7468–7472.
[38] A. Naghizadeh, R. Nabizadeh, Removal of reactive blue 29 dye with modified chitosan in presence of hydrogen peroxide, Environ. Prot. Eng., 42 (2016) 149–168.
[39] S.-g. Wang, W.-x. Gong, X.-w. Liu, B.-y. Gao, Q.-y. Yue, D.-h. Zhang, Removal of fulvic acids from aqueous solutions via surfactant modified zeolite, Chem. Res. Chin. Univ., 22 (2006) 566–570.
[40] K. Khalatbari, S. Bazgir, Evaluation of sulphate adsorption by nanostructure LDH (in Persian), J. Min. Eng., 8 (2013) 35–39.
[41] M.T. Sulak, E. Demirbas, M. Kobya, Removal of Astrazon Yellow 7GL from aqueous solutions by adsorption onto wheat bran, Bioresour. Technol., 98 (2007) 2590–2598.
[42] A. Naghizadeh, H. Shahabi, F. Ghasemi, A. Zarei, Synthesis of walnut shell modified with titanium dioxide and zinc oxide nanoparticles for efficient removal of humic acid from aqueous solutions, J. Water Health, 14 (2016) 989–997.
[43] M.H. Dehghani, A. Naghizadeh, A. Rashidi, E. Derakhshani, Adsorption of reactive blue 29 dye from aqueous solution by multiwall carbon nanotubes, Desal. Wat. Treat., 51 (2013) 7655–7662.
[44] A. Asfaram, M.R. Fathi, Removal of Direct Red 12B dye from aqueous solutions by wheat straw: isotherms, kinetics and thermodynamic studies, J. Color Sci. Technol., 1419 (2012) 19–15.
[45] S. Vasudevan, J. Lakshmi, The adsorption of phosphate by graphene from aqueous solution, RSC Adv., 2(2012) 5234–5242.
[46] P. Ganesan, J. Lakshmi, G. Sozhan, S. Vasudevan, Removal of manganese from water by electrocoagulation: adsorption, kinetics and thermodynamic studies, Can. J. Chem. Eng., 91 (2013) 448–458.
[47] S. Bagherifam, A. Lakzian, M. Rezaei, Uranium removal from aqueous solutions by iranian natural zealite – riched clinoptiolite (in Persian), Water. Soil (Agric. Sci. Technol.), 24 (2010) 19–24.
[48] M.T. Ghanian, M.T.H. Alizadeh, G. Ghanizadeh, M.H. Ehrampoush, Analytical survey of the kinetics and thermodynamics of phosphate adsorption from aqueous solutions using bone charcoal (in Persian), Mil. Med., 16 (2015) 183–189.
[49] W. Cao, Z. Dang, X.-Q. Zhou, X.-Y. Yi, P.-X. Wu, N.-W. Zhu, G.-N. Lu, Removal of sulphate from aqueous solution using modified rice straw: preparation, characterization and adsorption performance, Carbohydr. Polym., 85 (2011) 571–577.
[50] R. Kamaraj, P. Ganesan, S. Vasudevan, Removal of lead from aqueous solutions by electrocoagulation: isotherm, kinetics and thermodynamic studies, Int. J. Environ. Sci. Technol., 12 (2015) 683–692.
[51] H. Runtti, T. Luukkonen, M. Niskanen, S. Tuomikoski, T. Kangas, P. Tynjälä, E.T. Tolonen, M. Sarkkinen, K. Kemppainen, J. Rämö, U. Lass, Sulphate removal over barium-modified blast-furnace-slag geopolymer, J. Hazard. Mater., 317 (2016) 373–384.
[52] S. Vasudevan, J. Lakshmi, G. Sozhan, Studies on the Al–Zn–In-alloy as anode material for the removal of chromium from drinking water in electrocoagulation process, Desalination, 275 (2011) 260–268.
[53] S. Vasudevan, J. Lakshmi, R. Kamaraj, G. Sozhan, A critical study on the removal of copper by an electrochemically assisted coagulation: equilibrium, kinetics, and thermodynamics, Asia-Pac. J. Chem. Eng., 8 (2012) 162–171.
[54] H. Runtti, P. Tynjala, S. Tuomikoski, T. Kangas, T. Hu, J. Rama, U. Lassi, Utilisation of barium-modified analcime in sulphate removal: isotherms, kinetics and thermodynamics studies, J. Water Process Eng., 16 (2017) 319–328.